Phase-modulation effects in self-diffraction

Qiguang Yang, Jinhai Si, Yougui Wang, and Peixian Ye*
Institute of Physics, Chinese Academy of Sciences, P.O. Box 603, Beijing 100080, People's Republic of China
(Received 14 March 1996)

Phase-modulation effects in self-diffraction with two pump beams incident on a nonlinear medium were studied theoretically and experimentally. Based on a two-level model and considering the influence of the phase modulation on the phase matching, expressions describing the first-order and second-order scattered intensities were derived. The influences of phase modulation on the pump-intensity dependence and the sample-concentration dependence of the scattered intensities were discussed via numerical calculations. Experiments were performed with tetrahydrofuran solution of 1,4-diethinyl benzene to demonstrate the theoretical results. Some interesting results predicted by the theory, such as the fact that the scattered intensities of the sample with lower concentration can be larger than that with higher concentration at suitable high intensity of the pump, have been observed. [S1050-2947(96)06808-4]

PACS number(s): 42.65.Hw

I. INTRODUCTION

In terms of nonlinear optics, self-diffraction, in which two coherent light waves interact and produce scattered waves, is a well-known nonlinear wave mixing process [1,2]. In the grating approach, this process may also be seen as the read-out of the purely sinusoidal or nonsinusoidal modulation of the refractive index of a material written by two pump beams [3,4]. This kind of light-induced grating has been used as a powerful tool for the investigations of spectroscopy and relaxation dynamics [5,6]. A lot of experiments, such as forward phase conjugation, beam amplification, ultrafast relaxation processes and saturation spectroscopy, etc., have been performed in the self-diffraction regime.

Perturbative approaches have been used in the theoretical treatments of self-diffraction, although they are not strictly valid for the studies of saturable absorbers near resonance. Fragnito *et al.* developed a nonperturbative approach for the population gratings created in a saturable absorber [7,8]. This theory was applied to the self-diffraction in rhodamine 6G-doped boric acid glass by Kumar *et al.* [9]. Recently, Divakara Rao and Sharma extended this theory to the studies of diffraction of a third beam at an arbitrary incident angle from the grating written by two coherent pump beams [10]. All of these treatments, however, neglected the self- and cross-phase modulation effects of the laser beams; namely, the phase mismatchings and/or the coherence lengths for the interactions were considered to be independent on the pump-beam intensity. From the experimental point of view, one is especially interested in the case of two strong incident waves. Under this condition, the intensity-dependent refractive index changes, which influence the phase-matching condition, should not be neglected. This fact has been reflected in the weak beam amplification experiments via forward degenerate optical wave mixing in the local response nonlinear medium, in which the gain of the weak beam was demonstrated theoretically by Khoo and co-workers to be coming from the third-order wave mixing processes of the generated waves and the pump waves [11–15]. It has been shown that the gain factor of the interaction is substantially reduced by the phase mismatching, but the intensity-dependent phase modulation effects can compensate for this phase mismatching, leading to a phase-matched weak beam amplification process and an appreciable gain enhancement. That is to say, phase-modulation effects may play an important role in self-diffraction.

In this paper, we treat the self-diffraction problems where the two incident beams have equal and rather strong intensities. Therefore, the high-order scattered waves were generated not only from the third-order wave mixing, but also, and mainly, from the nonsinusoidal components of the index grating written by the incident waves. In particular, we emphasize how the intensities of the scattered waves and their intensity ratios are affected by the intensity-dependent phase modulation. In the theoretical section, a two-level model is adopted for the nonlinear medium, and operation in a nearly resonant wavelength is assumed. From the Fourier expansion of the macroscopic electric polarization of the medium, we obtained the radiation sources of the mth scattered waves. Then the analytical expressions for the first- and the second-order scattered intensities in the limit of small depletion of the pump beams were derived when only two Fourier components were dominant. The roles of various factors such as the pump-beam intensity, the linear absorption or the concentration of the sample, the detuning parameter, the thickness of the sample, and the crossing angle of the pump beams in the nonlinear medium in self-diffraction are clearly identified. The interesting results are discussed. In the last section, our experimental results are presented, which preliminarily demonstrate the theoretical predictions in limited regions of the pump-beam intensity and the sample concentration.

II. THEORY

Consider two coherent plane waves with identical polarization and equal amplitudes, $\widetilde{E}_0^+=\widetilde{E}_0^-=\widetilde{E}_0$, crossing at a small angle (2θ) in the nonlinear media with wave vectors

*Fax: (86)-10-62562605. Electronic address: user303@aphy01.iphy.ac.cn

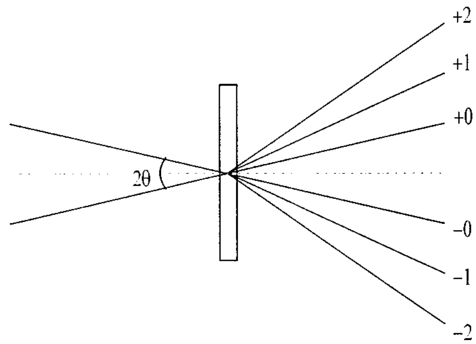

FIG. 1. Geometry for studies of self-diffraction where two pump beams make a small angle 2θ.

$\mathbf{k}_0^+$ and $\mathbf{k}_0^-$, as is sketched in Fig. 1. The total field in the medium can be written as

$$E = E_0 + \delta E = \sum_{m=0}^{\infty} E_m \cos\left(\frac{2m+1}{2}\kappa x\right), \tag{1}$$

where $\kappa = |\mathbf{k}_0^+ - \mathbf{k}_0^-| = (4\pi/\lambda)\sin(\theta)$, $E_m = \widetilde{E}_m e^{-ik_{mz}z}$, with $k_{mz} = (\omega/c)[n_0^2 - (2m+1)^2 \sin^2\theta]^{1/2}$. $\mathbf{k}_m^\pm$ is the wave vector of the $\pm m$th scattered waves, λ is the wavelength of the pump beam, n_0 is the linear refractive index of the sample (including the contributions of the solute and the solvent), E_0 represents the pump wave, and δE represents the scattered waves.

This field must satisfy Maxwell's wave equation

$$\nabla^2 E + \frac{\omega^2}{c^2} n_0^2 E = -\mu_0 \omega^2 P^{\mathrm{NL}}, \tag{2}$$

where P^{NL} is the nonlinear polarization of the medium.

Assuming a two-level system characterized by a dipole moment μ and longitudinal and transverse relaxation times T_1 and T_2, the density matrix equations can be solved and the macroscopic polarization, $P(E)$ can be derived as a function of the optical field:

$$P(E) = -\frac{2\alpha_0\varepsilon_0}{k_0} \frac{(i+\delta)}{(1+\delta^2+|E/E_s|^2)} E \tag{3}$$

with the definitions

$$\delta = (\omega - \omega_0)T_2, \quad \alpha_0 = \frac{\mu^2 N T_2 k_0}{2\varepsilon_0 \hbar},$$

where α_0 is the line-center linear absorption coefficient, k_0 is the magnitude of the wave number at frequency ω, N is the molecule number per cubic meter, and $|E_s|^2$ is the line-center saturation "intensity" [16].

Consider the Fourier decomposition of the macroscopic polarization and divide the Fourier components into linear (P^{L}) and nonlinear (P^{NL}) parts; one may obtain

$$P^{\mathrm{L}} = -\frac{2\varepsilon_0\alpha_0}{k_0} \frac{i+\delta}{1+\delta^2} E,$$

$$\begin{aligned} P^{\mathrm{NL}} \approx ABI_s\Bigg(& AI_0 - 1 - 2I_0^2A^2 \\ & + \frac{2\varepsilon_0\alpha_0}{k_0}\frac{i+\delta}{1+\delta^2}\Bigg) E_0[e^{-i(k_{0z}z + k_{0x}^+ x)} + e^{-i(k_{0z}z + k_{0x}^- x)}] \\ & + A^2 B I_0 I_s (1 - AI_0) E_0 [e^{-i(k_{0z}z + k_{1x}^+ x)} + e^{-i(k_{0z}z + k_{1x}^- x)}] \\ & - A^3 B I_0^2 I_s E_0 [e^{-i(k_{0z}z + k_{2x}^+ x)} + e^{-i(k_{0z}z + k_{2x}^- x)}] + \cdots, \end{aligned} \tag{4}$$

with

$$A = \frac{1}{2I_0 + I_s(1+\delta^2)}, \quad B = \frac{2\varepsilon_0\alpha_0}{k_0}(i+\delta),$$

where $I_0 \propto |E_0|^2$ is the intensity of the incident beam, $I_s \propto |E_s|^2$, and $k^\pm{}_{mx} = k_{0x}^\pm \pm m\kappa = \pm(m+1/2)\kappa$ is the x component of the wave vector of the $\pm m$th-order scattered wave. Each term in Eq. (4) represents a source for a pair of waves that will emerge from the medium with wave vectors $\mathbf{k}^\pm{}_m = (k^\pm{}_{mx}, k_{mz})$. Substituting Eqs. (4) and (1) into Eq. (2) and assuming that the absorption $\alpha_0^\omega = \alpha_0/(1+\delta^2)$ at frequency ω is negligibly small, but maintaining the intensity-dependent phase changes, we can get the first- and the second-order scattered intensities as follows:

$$\begin{aligned} I^{(1)}(l) &= R^2 I_0 l^2 \operatorname{sinc}^2\left(\frac{\pi l}{l_{1c}}\right), \\ I^{(2)}(l) &= T^2 I_0^2 A^2 l^2 \operatorname{sinc}^2\left(\frac{\pi l}{l_{2c}}\right) \end{aligned} \tag{5}$$

with

$$R = \frac{k_0}{k_{1z}} \alpha_0 \sqrt{1+\delta^2} I_0 I_s A^2 (1 - AI_0),$$

$$T = \frac{k_0}{k_{2z}} \alpha_0 \sqrt{1+\delta^2} I_0^{3/2} I_s A^2,$$

$$l_{1c} = \frac{2\pi}{k_{0z} - k_{1z} - S \sin\varphi_\delta},$$

$$l_{2c} = \frac{2\pi}{k_{0z} - k_{2z} - S \sin\varphi_\delta},$$

$$\varphi_\delta = -\arctan g\,\delta,$$

$$S = \frac{k_0}{k_{0z}} \alpha_0 \sqrt{1+\delta^2} I_s A (AI_0 - 1 - 2I_0^2A^2) + \frac{k_0}{k_{0z}} \frac{\alpha_0\sqrt{1+\delta^2}}{1+\delta^2},$$

$$k_{mz} = \frac{\omega}{c}[n_0^2 - (2m+1)^2 \sin^2\theta]^{1/2}, \tag{6}$$

$$n_0 = \sqrt{\eta^2 - \frac{2\alpha_0\delta}{k_0(1+\delta^2)}},$$

where η is the linear refractive index of the solvent and l is the thickness of the sample.

To get these results, we have used the slowly varying amplitude approximation, and assumed that the scattered-wave amplitudes are small compared with those of the pump beams, thereby the cascade effect was neglected.

We notice that the factor $S\ \sin\varphi_\delta$ that appeared in the coherent lengths l_{1c} and l_{2c} depends on the pump-beam intensity and represents the influences of the intensity-dependent phase-modulation. From Eq. (5), we find that the scattered intensity grows with I_0^{2m+1} when $I_0 \ll I_s$, and decreases with $1/I_0$ when $I_0 \gg I_s$. This is consistent with the previous treatments.

It can be seen from Eq. (6) when the phase-modulation effects were taken into account, that the coherent lengths l_{1c}, l_{2c} of the scattered processes, which characterize the propagation distances within the nonlinear medium over which phase-matching conditions are maintained approximately, will not only depend on the cross angle, the wavelength and the linear refractive index, but also on the intensities of the pump beams.

In other words, in this case the effective phase mismatching $\Delta k_{1,\mathrm{eff}} = (k_{0z} - k_{1z} - S\ \sin\varphi_\delta)$ and $\Delta k_{2,\mathrm{eff}} = (k_{0z} - k_{2z} - S\ \sin\ \varphi_\delta)$, which are inversely proportional to l_{1c} and l_{2c}, will be intensity dependent. Therefore, the scattered intensities related to the incident intensity in this system will be significantly different from that in the system with intensity-independent phase mismatching $\Delta k_1 = (k_{0z} - k_{1z})$ and $\Delta k_2 = (k_{0z} - k_{2z})$.

If the interaction length and/or the cross angle of the two pump beams are small enough for the intensity-independent phase-matching condition to be approximately satisfied, $\Delta k_1 = (k_{0z} - k_{1z}) \approx 0$, $\Delta k_2 = (k_{0z} - k_{2z}) \approx 0$, part of intensity-dependent phase mismatching $-S\ \sin\varphi_\delta$ may change this condition, leading to the decrease of scattered intensities. This influence is sketched in Fig. 2, where the results are obtained on the assumption that the cross angle of the pump beams is 1 mrad, the thickness of the sample $l = 1$ mm, so $\Delta k_1 = 0$ is approximately satisfied. In this figure, intensities of the first-order scattering as a function of pump-beam intensity, calculated by Eq. (5) when considering the intensity-dependent phase mismatching, are shown by solid curves for $\alpha_0^\omega = 2.4$ and $1.2\ \mathrm{cm}^{-1}$, respectively. For comparison, also shown, by the dashed curves, are those calculated when the phase-modulation effect removed. An evident decrease of the scattered intensity for the case considering the intensity-dependent phase modulation can be observed when the pump intensity is strong enough, particularly for $\alpha_0^\omega = 2.4\ \mathrm{cm}^{-1}$. The other parameters used in Fig. 2 are $\eta = 1.4$, $\delta = 20$, $I_s = 2.5 \times 10^7\ \mathrm{W/m}^2$.

If Δk_1 (or Δk_2) $\neq 0$ and $S\ \sin\ \varphi_\delta$ are positive, then with the increase of the pump intensity, $S\ \sin\ \varphi_\delta$ changes also. When $S\ \sin\varphi_\delta \leq \Delta k_1$ (or Δk_2), the intensity-independent phase mismatching can be compensated by $S\ \sin\ \varphi_\delta$ and the scattered intensities can become larger, but when $S\ \sin\ \varphi_\delta > \Delta k_1$ (or Δk_2), the intensity-dependent phase mismatching can make $\Delta k_{1,\mathrm{eff}}$ (or $\Delta k_{2,\mathrm{eff}}$) become larger than Δk_1 (or Δk_2), and the scattered intensities can become smaller. These results are indicated in Figs. 3 and 4, where data used for the calculation are the detuning parameter $\delta = -20$, the saturate intensity $I_s = 2.5 \times 10^7\ \mathrm{W/m}^2$, the cross angle of the two pump beams are $2\theta = 2.6 \times 10^{-2}$ rad, the thickness of the sample $l = 2$ mm, and the linear refractive index of the solvent is $\eta = 1.4$. Figure 3 shows the phase-mismatching factor $\sin c^2(\pi l / l_{1c})$ as a function of the pump intensity calculated by Eq. (6) for two cases: $\alpha_0^\omega = 1.2\ \mathrm{cm}^{-1}$ and $\alpha_0^\omega = 2.4\ \mathrm{cm}^{-1}$. When the pump intensity is small, this factor is determined essentially by the intensity-independent mismatching. With the increase of the pump intensity, it begins to increase, which means the intensity-independent mismatching begins to be compensated by $S\ \sin\varphi_\delta$. When the pump intensity increases further, it drops for the case $\alpha_0^\omega = 2.4\ \mathrm{cm}^{-1}$ after going through a maximum, which corresponds to the effective phase-

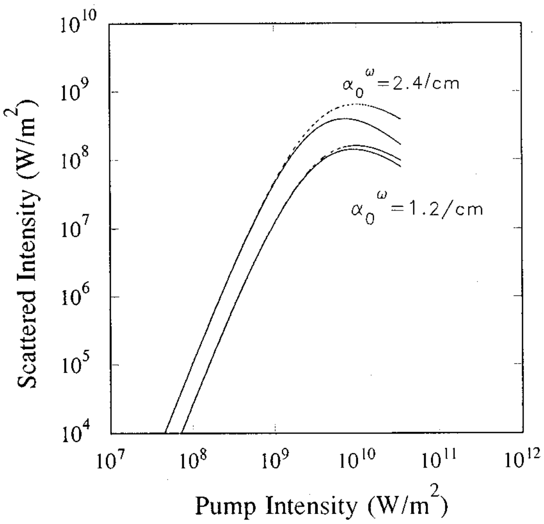

FIG. 2. First-order scattered intensities as functions of the pump intensity when the intensity-independent phase-matching condition is satisfied, are shown with solid curves. Dashed curves describe the theoretical results with the phase-modulation effect removed. The parameters used in the calculation are $\delta = 20$, $\theta = 1$ mrad, $\eta = 1.4$, $l = 1$ mm, and $I_s = 2.5 \times 10^7\ \mathrm{W/m}^2$.

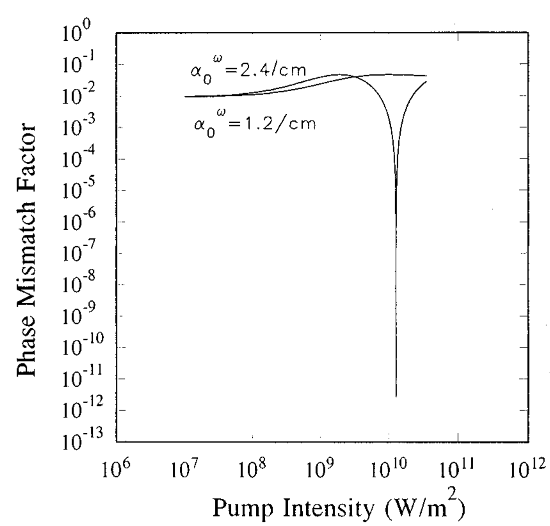

FIG. 3. Phase-mismatching factor $\sin c^2(\pi l / l_{lc})$ as a function of the pump intensity for $\alpha_0^\omega = 1.2$ and $2.4\ \mathrm{cm}^{-1}$. The other parameters used in the calculation are $\delta = -20$, $\eta = 1.4$, $I_s = 2.5 \times 10^7\ \mathrm{W/m}^2$, $l = 2$ mm, and $\theta = 0.013$ rad.

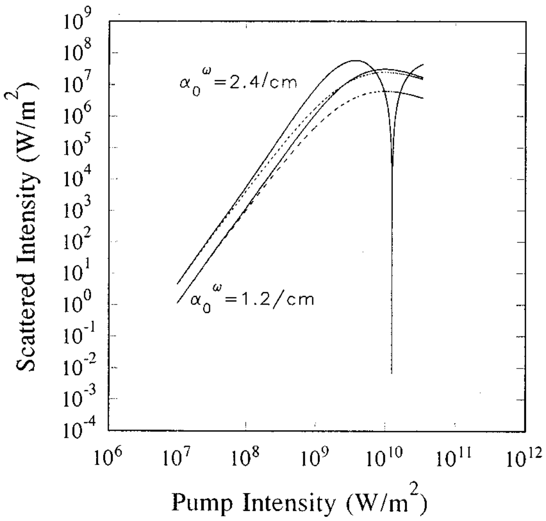

FIG. 4. First-order scattered intensities as functions of the pump intensity, shown with solid curves. The theoretical results with the phase-modulation effects removed are shown by the dashed curves. The parameters used in the calculation are the same as Fig. 3.

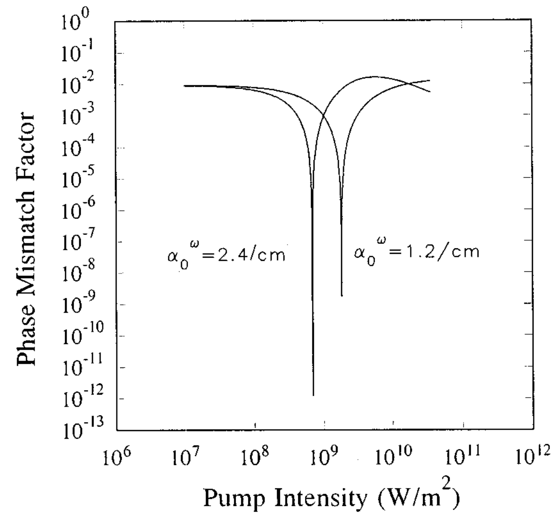

FIG. 5. Phase-mismatching factor $\sin c^2(\pi l/l_{1c})$ is a function of the pump intensity for α_0^ω=1.2 and 2.4 cm^{-1}. The other parameters used in the calculation are δ=20, η=1.4, I_s=2.5×10^7 W/cm^2, l=2 mm, and θ=0.013 rad.

mismatching increases after the intensity-independent mismatching is compensated completely. Figure 4 shows the first-order scattered intensity as a function of the pump intensity, calculated by Eq. (5) for the above two cases, with solid curves. The results, without taking into account the phase-modulation effect are also shown by the dashed curves for comparison. When the pump intensity is small, the solid and the dashed curves are consistent, but with the increase of the pump intensity the values shown by solid curves begin to be larger than those shown by the corresponding dashed curves, which reflects that the intensity-independent mismatching begins to be compensated, consistent with what has been shown in Fig. 3. When the pump intensity increases further, corresponding to the fact indicated in Fig. 3 that the effective phase mismatching increases after a complete compensation of the intensity-independent phase mismatching, the value shown by the solid curve for α_0^ω=2.4 cm^{-1} becomes smaller than that shown by the corresponding dashed curve after arriving at a maximum. We can imagine that the same phenomenon will occur for the case of α_0^ω=1.2 cm^{-1} if the pump intensity increases to a high enough level. It is worthwhile noting that in some regions of pump intensity in Fig. 4, the scattered intensity in the case of α_0^ω=1.2 cm^{-1} can be larger than that of α_0^ω=2.4 cm^{-1}. That is to say, the scattered intensity of the sample with lower concentration can be larger than that with higher concentration for some suitable intensities of the pump beam when the phase modulation is considered.

In contrast to the positive light-induced phase mismatching, $S \sin\varphi_\delta$, the negative $S \sin\varphi_\delta$ will always make the effective phase mismatching larger, so that with an increase of the pump intensity, the phase-modulation effect decreases the scattered intensity until it reaches the first minimum. As the pump intensity increases further, another maximum value of $\sin c^2(\pi l/l_{1c})$ will be approached, and the scattered wave intensities will gradually increase and then decrease again when $\sin c^2(\pi l/l_{1c})$ begins to reduce again. The phase-mismatching factor $\sin c^2(\pi l/l_{1c})$ as a function of the pump intensity is plotted in Fig. 5. The parameters in Figs. 5 and 6 are the same as those in Figs. 3 and 4, except that δ=20. We find that the phase-mismatching factor changes more quickly with pump intensity when α_0^ω is larger, and in some scope of the pump intensity, the phase-mismatching factor of the sample with smaller α_0^ω may be larger than that of the sample with larger α_0^ω. Figure 6 shows the first-order scattered intensity calculated as a function of pump intensity with solid curves for the corresponding cases of Fig. 5, and the dashed lines represent the theoretical results obtained with the phase-modulation effect removed. We can see that before the

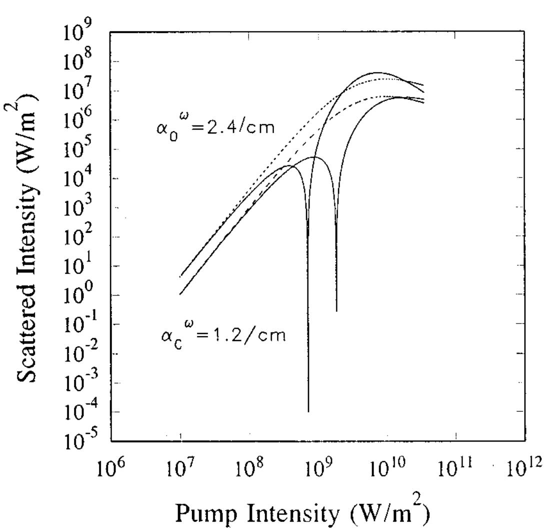

FIG. 6. First-order scattered intensities as functions of the pump intensity, shown by solid curves. The theoretical results with the phase-modulation effect removed are shown with dashed curves. The parameters used in the calculation are the same as in Fig. 5.

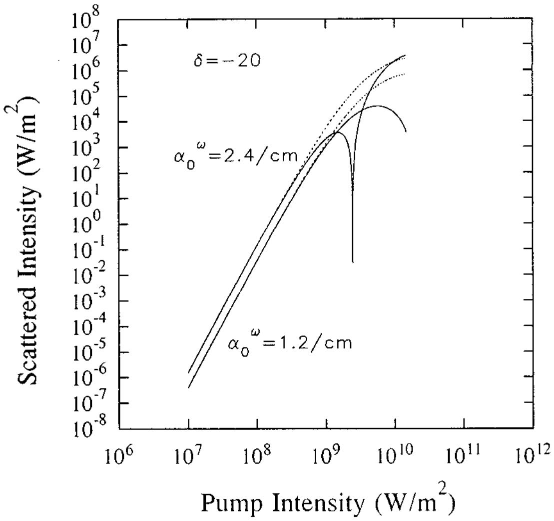

FIG. 7. Second-order scattered intensities as functions of the pump intensity, shown with solid curves. The theoretical results with phase-modulation effect removed are shown by dashed curves. The parameters used in the calculation are the same as in Fig. 4.

first minimum is reached, the scattered intensities shown by the solid curves are always smaller than those shown by the corresponding dashed curves, but after that, the former can be larger than the latter in some regions of pump intensity.

The characters of the second-order scattered wave, as depicted in Figs. 7 and 8, are analogous to those of the first-order scattered wave. Notice that the intensity-independent phase mismatching of this order is nearly 11 times that of $\pi/2$, which approximately corresponds to one of the maxima of the intensity-independent phase-mismatching factor; then the decrease of the scattered intensities when the phase-modulation effect is taken into account regardless of positive

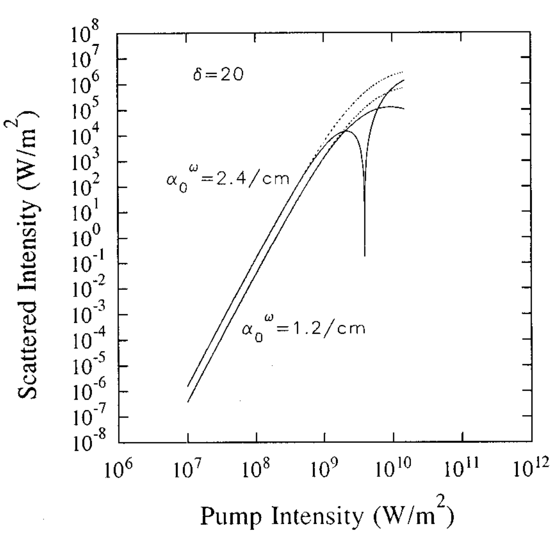

FIG. 8. Second-order scattered intensities as functions of the pump intensity, shown by solid curves. The theoretical results with the phase-modulation effect removed are shown by the dashed curves. The parameters used in the calculation are the same as in Fig. 6.

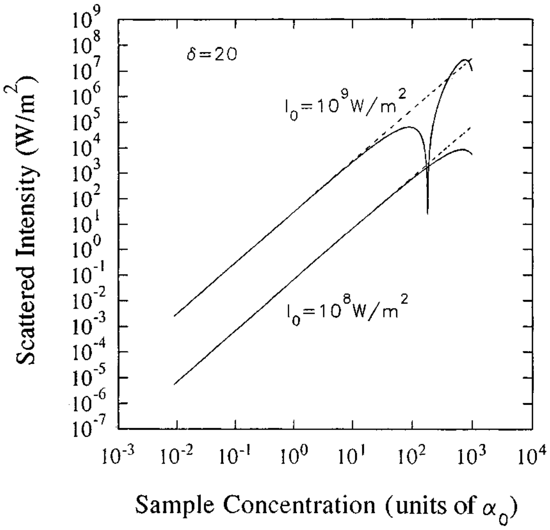

FIG. 9. First-order scattered intensities as functions of the linear absorption α_0^{ω}, which is proportional to the concentration of the sample, shown by solid curves. The theoretical results with the phase-modulation effect removed are shown by the dashed curves. The other parameters used in the calculation are the same as in Fig. 6.

or negative δ, as shown in Figs. 7 and 8, can be understood. The parameters used in Figs. 7 and 8 are the same as in Figs. 4 and 6, respectively.

The factor $S \sin \varphi_{\delta}$ depends not only on the pump intensity but also on the linear absorption coefficient α_0^{ω}, as can be seen from Eq. (6), so that not only the pump intensity but also the concentration N of the sample (note: $\alpha_0^{\omega} \propto N$) can change the effective phase mismatching and influence the scattered intensity. As an example, the first-order scattered wave intensity as a function of the linear absorption α_0^{ω} at two different pump intensities is calculated and shown in Fig. 9 by solid curves. The dashed lines in the figure represent the corresponding results calculated with the phase-modulation effect removed. The other parameters used in the calculations are the same as used in Fig. 6.

It should be noted that the theoretical treatment of phase-modulation effects in self-diffraction presented in this paper are limited to the steady-state condition. However, this condition can also be satisfied when the duration of the laser pulse is longer than the relaxation time of the sample excitation.

III. EXPERIMENTS

An experiment was designed to check the theoretical results. The nonlinear medium was chosen as 1,4-diethinyl benzene (in tetrahydrofuran, the linear refractive index of this solvent is $\eta=1.4$), the linear absorptions of the samples were about $0.01\sim2.4\ \mathrm{cm}^{-1}$. The thickness of the sample cell was $l=2$ mm.

The experiment was arranged according to the configuration of Fig. 1. The second-harmonic generation (SHG) of a Q-switched neodymium-doped yttrium aluminum garnet (Nd:YAG) laser with 8-ns-pulse width was used as the light source. The output beam with a wavelength of 532 nm was split into 2, with equal intensities, and used as the pump

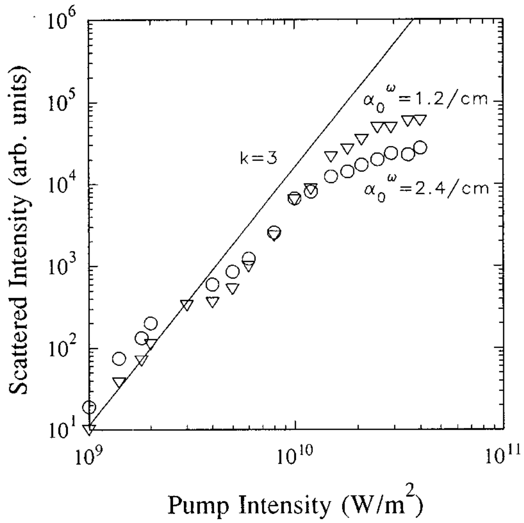

FIG. 10. Experimental results for the first-order scattered intensities as functions of the pump intensity when the concentration is fixed at $\alpha_0^\omega=1.2$ and 2.4 cm^{-1}. Parameters used are $\theta=0.013$ rad, $\eta=1.4$, and $l=2$ mm.

beams. They intersected in the sample cell with a beam diameter of about 0.2 mm. The cross angle 2θ of the two pump beams was about 0.026 rad.

We measured the scattered intensities as a function of pump intensity for the fixed sample concentration, and also those as a function of sample concentration for the fixed pump intensity. The results are shown respectively, in Figs. 10–12.

Figures 10 and 11 show the measured scattered intensities versus pump intensity, respectively, for the first- and the second-order scattered waves. Each point represents the average of 100 events. We find the pump-intensity dependencies of the scattered waves to be in agreement with the pre-

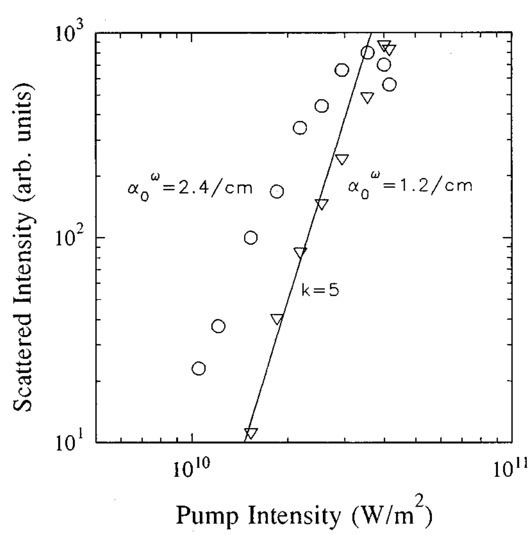

FIG. 11. Experimental results for the second-order scattered intensities as functions of the pump intensity when the concentration is fixed at $\alpha_0^\omega=1.2$ and 2.4 cm^{-1}. Parameters used are $\theta=0.013$ rad, $\eta=1.4$, and $l=2$ mm.

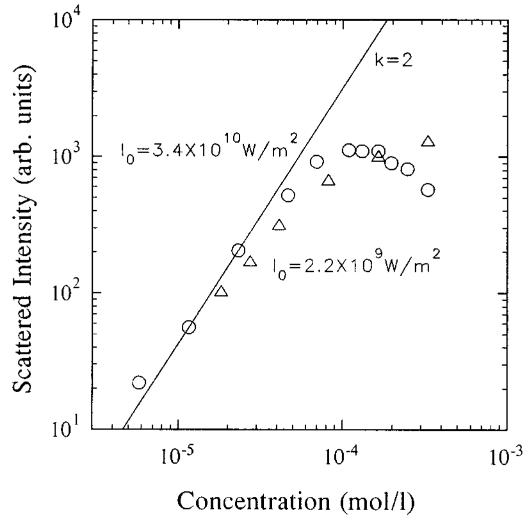

FIG. 12. Experimental results for the first-order scattered intensities as functions of the sample concentration when the incident intensity is fixed at $I_0=0.22\times10^{10}$ W/m^2 and $I_0=3.4\times10^{10}$ W/m^2. Parameters used are $l=2$ mm, $\theta=0.013$ rad, and $\eta=1.4$. The linear absorption α_0^ω is about 2.4 cm^{-1} when the concentration of the sample is 2.3×10^{-3} mol/l.

dicted behavior as shown in Figs. 4 and 8. When the pump intensity is small, a cubic dependence is expected for the first-order scattered wave, and thus we compare that with a line of slope 3 on the log-log plot in Fig. 10. For the second-order scattered wave, as shown in Fig. 11, we compare the results to a line of slope 5. As the pump intensity increases, the scattered intensities deviate from the straight lines due to the saturation effect, as well as the phase-modulation effect. Particularly, we notice that the scattered intensities of the sample with lower concentration become larger than those with higher concentration when the pump intensity is larger than about 10^{10} W/m^2 for the first-order scattering, and about 3×10^{10} W/m^2 for the second-order scattering. As we analyzed above, this result is due to the fact that the higher the concentration, the larger the light-induced phase mismatching.

Figure 12 shows the first-order scattered wave intensity as a function of the sample concentration at the pump intensities of $I_0=3.4\times10^{10}$ W/m^2 and $I_0=0.22\times10^{10}$ W/m^2, respectively. When the concentration of the sample is very small, the intensity-dependent phase mismatching could be neglected and the square dependence of the signal intensity on the concentration should be presented. This result can be obtained from Eq. (5) and was demonstrated in our experiments, as shown in Fig. 12. At higher concentration, the intensity-dependent phase mismatching will influence the scattered intensity significantly. If the effective phase mismatching of the interaction at higher pump intensity is larger than that at lower pump intensity, an interesting character of the scattered intensity should be presented; that is, for a sample with certain concentration, the scattered intensity will be larger at lower pump intensity, and smaller at higher pump intensity; this result is also shown in Fig. 12.

IV. CONCLUSION

This investigation has been devoted to the study of the phase-modulation effects in self-diffraction in nonlinear optical media. The theoretical model involving a two-level system has been developed and used to describe the scattered intensity when considering the influence of the phase modulation on the phase-matching condition. Analytical results have been obtained in the small linear absorption hypothesis, allowing us to understand the particular role played easily and clearly by the phase-modulation effect. Some interesting results, for example, at some suitable sample concentrations are that the scattered intensity is larger at lower pump intensity and smaller at higher pump intensity. On the other hand, at some suitable range of pump intensity, the scattered intensity is larger at lower concentration and smaller at higher concentration, and have been predicted by this theory and demonstrated by experiments. We believe that this study may be useful in helping readers to understand the physical mechanics of self-diffraction and other nonlinear effects.

ACKNOWLEDGMENTS

We would like to thank Professor Mujie Yang and her colleagues of Zhejiang University in China for their supporting of experimental samples. This research was supported by the National Natural Science Foundation of China.

[1] T. Yajima and H. Souma, Phys. Rev. A **17**, 309 (1978).
[2] C. V. Heer and N. C. Griffen, Opt. Lett. **4**, 239 (1979).
[3] A. Von Jena and H. E. Lessing, Opt. Quantum Electron. **11**, 419 (1979).
[4] L. J. Rothberg and N. Bloembergen, Phys. Rev. A **30**, 2327 (1984).
[5] F. Keilman, Appl. Phys. **14**, 29 (1979).
[6] D. W. Phillion, D. J. Kuizenga, and A. E. Siegman, Appl. Phys. Lett. **27**, 85 (1975).
[7] H. L. Fragnito, S. F. Pereira, and A. Kiel, J. Opt. Soc. Am. B **4**, 1309 (1987).
[8] H. L. Fragnito, S. F. Pereira, and A. Kiel, Opt. Lett. **11**, 27 (1986), and references therein.
[9] G. R. Kumar, B. P. Siagh, and K. K. Sharma, J. Opt. Soc. Am. B **8**, 2119 (1991).
[10] K. Divakara Rao and K. K. Sharma, J. Opt. Soc. Am. B **12**, 658 (1995).
[11] I. C. Khoo and T. H. Liu, Phys. Rev. A **39**, 4036 (1989).
[12] I. C. Khoo and Ping Zhou, Phys. Rev. A **41**, 1544 (1990).
[13] H. J. Eichler, M. Glotz, A. Kummrow, K. Richter, and X. Yang, Phys. Rev. A **35**, 4673 (1987).
[14] T. H. Liu and I. C. Khoo, IEEE J. Quantum Electron. **QE-23**, 2020 (1987).
[15] F. Sanchez, J. Opt. Soc. Am. B **9**, 2196 (1992).
[16] R. L. Abrams and R. C. Lind, Opt. Lett. **2**, 94 (1978).